Phonons and Heat Capacity of Polyoxymethylene

Shweta Srivastava,[1] Seema Srivastava,[1] Shinoo Srivastava,[2] Sanjeev John La'Verne,[3] Irfan Ali Khan,[1] Parvez Ali,[1] V. D. Gupta[1]

[1]*Department of Physics, Integral University, Lucknow 226026, Uttar Pradesh, India*
[2]*Department of Physics, College of Engineering Science and Technology Lucknow, Uttar Pradesh, India*
[3]*Department of Physics, Lucknow Christian College, Lucknow, Uttar Pradesh, India*

Received 16 January 2009; accepted 27 December 2010
DOI 10.1002/app.34050
Published online 23 May 2011 in Wiley Online Library (wileyonlinelibrary.com).

ABSTRACT: Using Wilson's GF matrix method as modified by Higgs for an infinite system, we report normal modes and their dispersion for polyoxymethylene using the Urey-Bradley force field. Heat capacity has been evaluated as a function of temperature from dispersion curves via density-of-states. The results obtained agree well with the experimental data reported in the literature. © 2011 Wiley Periodicals, Inc. J Appl Polym Sci 122: 1376–1381, 2011

Key words: polyoxymethylene; heat capacity; density-of-states; dispersion curves

INTRODUCTION

Polyoxymethylene (POM)-(—O—CH_2—)$_n$—commonly known as Delrin is a polymer of formaldehyde and is the first member of the polyether series. It has a melting point of (180°C) and density (1.40–1.45 g/cc). Its structure is shown in Figure 1. It is often marketed and used as a metal substitute. It is a lightweight, low-friction, and wear-resistant thermoplastic with good physical and processing properties and capable of operating at temperatures in excess of 90°C. It is commonly used in the food industry, paintball markers, to make frame sliders and knee pucks for motorcycle riders as well as for slide gloves used when long boarding. It is made from acetal homopolymer resin, and, when extruded into large basic shapes (i.e., sheets, rods, and tubes), tends to be porous. Its low cost, adequate strength, light weight, and self-lubricating properties make it ideal for markers. Delrin has also recently found use in the manufacturing of Irish flutes (traditionally made of wood), tin whistles (traditionally made of metal), and bagpipes (traditionally made of wood). Delrin has become an increasingly popular material in the fabrication of picks. Due to large industrial advantages of POM, it has been extensively studied by a large number of workers.[1–20] In this communication, the sample purchased from sigma chemicals U.S.A, was annealed at 170°C and slow cooled to room temperature (1°C per 10 min). Detailed structure analysis of POM has been carried out by Uchida and Tadokoro.[6] They have reported the structural parameters according to which the bond distance C—O = 1.42 Å, the angle (COC = 112° 24′ and (OCO = 110° 49′. All internal rotation angles of the skeletal bonds are reported equal to 78°13′. It is further predicted that each crystallite of POM is composed of only one type of helix either right or left handed. Dasgupta et al.[9] have developed a vibrationally accurate force field for molecular dynamics simulations of POM polymers. This force field was developed using the biased Hessian with singular value decomposition method (BH/SVD) applied to dimethyl ether and dimethoxymethane. The resultant force field contains parameters that were needed for molecular dynamics simulations of POM. Charges were derived from the electrostatic potential derived point charge calculations. The full *ab initio* (HF/6-31g) torsional potential energy fitted surface was fit using a Fourier series expansion to accommodate the anomeric effect in dimethoxymethane.

In view of its multifarious applications, POM is an important industrial polymer and deserves a detailed study of its dynamical behavior. Several such studies have been reported in the literature[7,13] but they are limited in scope and interpretation, for example thermodynamic studies such as heat capacity and density-of-states are not included. In this communication, we report a complete normal mode analysis of poloxymethylene, using Urey-Bradley force field. Phonon dispersion and heat capacity are obtained via the density-of-states derived from dispersion curves. The calculated heat

Correspondence to: V. D. Gupta (vdgupta24@rediffmail.com).

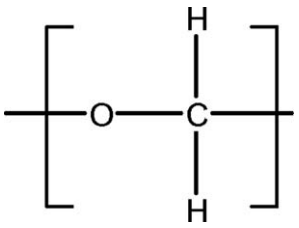

Figure 1 Chemical repeat unit of polyoxymethylene.

capacity has been compared with experimental results of Wunderlich et al.[8]

THEORY

Calculation of normal mode frequencies

The calculation of normal mode frequencies has been carried out according to the well known Wilson's GF[21] matrix method as modified by Higgs.[22] It consists of writing the inverse kinetic energy matrix G and the potential energy matrix F in terms of internal coordinates R. In case of an infinite isolated helical polymer, there are an infinite number of internal coordinate that lead to G and F matrices of infinite order. Due to the screw symmetry of the polymer, a transformation similar to that given by Born and Von Karman can be performed that reduces the infinite problem to finite dimensions.[23] The vibrational secular equation, which gives normal mode frequencies and their dispersion as a function of phase angle, has the form:

$$|G(\delta)F(\delta) - \lambda(\delta)I| = 0, \quad 0 \leq \delta \leq \pi \tag{1}$$

The vibrational frequencies $\nu(\delta)$ (in cm^{-1}) are related to the eigenvalues $\lambda(\delta)$ by the following relation:

$$\lambda(\delta) = 4\pi^2 c^2 \nu^2(\delta) \tag{2}$$

where, c is velocity of light.

Calculation of specific heat

Dispersion curves can be used to calculate the specific heat of a polymeric system. For an one-dimensional system, the density-of-state function or the frequency distribution function which expresses the way energy is distributed among various branches of normal modes in the crystal, is calculated from the relation:

$$g(\nu) = \Sigma_j (\partial v_j / \partial \delta)^{-1}|_{\nu j(\delta)=\nu} \tag{3}$$

with $\int_g (\nu_j)\, d\nu_j = 1$

The sum is over all branches j. Considering a solid as an assembly of harmonic oscillators, the frequency distribution $g(\nu)$ is equivalent to a partition function. The constant volume heat capacity C_v can be calculated using Debye's relation:

$$C_v = \Sigma_j g(\nu_j) k N_A (h\nu_j/kT)^2 \frac{\exp(h\nu_j/kT)}{[\exp(h\nu_j/kT) - 1]^2} \tag{4}$$

where, $g(\nu)$—density-of-states
k—Boltzmann constant
N—Avogadro number
T—Absolute temperature
h—Planck's constant

The constant volume heat capacity C_v, given by Eq. (4) is converted into constant pressure heat capacity C_p using the Nernst-Lindemann approximation.[23,24]

$$C_p - C_v = 3RA_o(C_p^2 T / C_v T_m^0) \tag{5}$$

where A_o is a constant often of a universal value [3.9×10^{-9} (kmol/J)] and T_m^0 is the equilibrium melting temperature.

Experiment

The FTIR spectra of the POM in the range 4000–400 cm^{-1} were recorded on an 8201 PC Fourier Transform IR spectrophotometer. Before running the spectra, the equipment chamber was well purged with dry nitrogen to avoid any confusion arising from water vapor peaks. The samples were in the solid state and the spectra were obtained in CsBr pellets. The spectra obtained in the range 4000–400 are shown in Figure 2.

RESULTS AND DISCUSSION

The structure of POM was determined by using the molecular modeling technique using CS-Chemdraw. It consists of calculating interatomic distances of all atoms over all possible ranges of dihedral angles. One then selects a set of contact distances which are fully allowed and another which is considered as minimal. The fully allowed contact distances result in fully allowed regions of the conformational plane. Thus all unfavorable steric overlaps are excluded from consideration. The molecular structure obtained by molecular modeling is also confirmed by the geometric parameters reported by Uchida and Tadokoro[6] from x-ray diffraction analysis. The cartesian coordinates obtained are given in Table I. They can be compared with those obtained from molecular modeling.

The number of atoms per residue —(—CH_2—O—)— in POM is four and hence there would be $(4 \times 3) - 4 = 8N$ modes of vibrations and 12 dispersion curves.

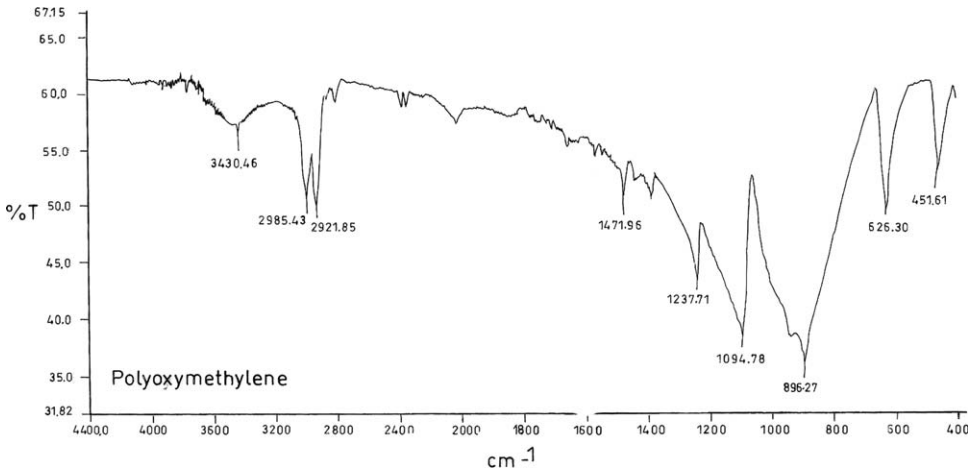

Figure 2 FTIR of polyoxymethylene in the range 4000–400 cm^{-1}.

The vibrational frequencies have been calculated for values of δ varying from 0 to π in steps of 0.05π. The optically active modes are those for which δ = 0, φ, 2φ. The four zero frequencies correspond to acoustic modes, three representing translations along the three axes and one is rotation around the chain axis.

The assignments were made on the basis of potential energy distribution (PED), band position, band shape, band intensity, and absorption/scattering in similar molecules having groups placed in similar environments. The Urey Bradley force constants were initially transferred from the earlier work on molecules having similar groups and were further refined by using the least-square method as described earlier. The final sets of force constants for POM are given in Table II. Except for a couple of frequencies, most of the frequencies are fitted within less than 1%. As mentioned earlier, the modes corresponding to δ = 0.0 are both Raman and IR active because they are totally symmetric and both dipole moment and polarizability component have non zero value under symmetry transformation. Therefore, the calculated frequencies are first fitted to the observed frequencies for this phase value. All vibrational modes along with their PED are given in Table III. The dispersion curves below 1600 cm^{-1} are shown in Figure 3(a). The modes showing specific features of dispersion curves are shown in Table IV.

TABLE I
Cartesian Coordinates

	X		Y		Z
1	.000000000000000D+00	1	.000000000000000D+00	1	.000000000000000D+00
2	.141000000000000D+01	2	.000000000000000D+00	2	.000000000000000D+00
3	.176459989788217D+01	3	−.457912824634077D+00	3	.815214546887871D+00
4	.166381567538202D+01	4	−.491029360965363D+00	4	−.833347328309341D+00
5	.189498456323580D+01	5	.133248413627442D+01	5	.000000000000000D+00
6	.181974383908380D+01	6	.192555104665356D+01	6	−.128692325848996D+01
7	.959385239660173D+00	7	.168720908867290D+01	7	−.173745204942764D+01
8	.188206762852824D+01	8	.290906787103865D+01	8	−.111718698829193D+01
9	.287789464918953D+01	9	.146085398260290D+01	9	−.209468157737952D+01
10	.410335372847130D+01	10	.210444052039628D+01	10	−.178683354120422D+01
11	.421212581228225D+01	11	.220558238669717D+01	11	−.797925579529020D+00
12	.480725248420027D+01	12	.150750789499271D+01	12	−.217179845182858D+01
13	.412990706001753D+01	13	.339152477093005D+01	13	−.236199356468613D+01
14	.441336550088559D+01	14	.334740572532194D+01	14	−.374250246437323D+01
15	.392380046096361D+01	15	.259378423480014D+01	15	−.418111473131283D+01
16	.410833488145972D+01	16	.423303282004792D+01	16	−.409267523644423D+01
17	.579419077851089D+01	17	.314647659773642D+01	17	−.394510808709565D+01
18	.653393824541951D+01	18	.433164777136106D+01	18	−.375473221044247D+01
19	.674868673328767D+01	19	.338104362303805D+01	19	−.353060090930532D+01
20	.747509377341102D+01	20	.402377535837623D+01	20	−.361530176378924D+01
21	.641244536772445D+01	21	.516309037404693D+01	21	−.488700544562394D+01
22	.723353843699914D+01	22	.473226807505017D+01	22	−.594921932158122D+01

TABLE II
Force Constant in (md/cm^{-1}) and Internal Coordinates of Polyoxymethylene

Bond	Force constant value	
	Bonded	Nonbonded
ν (C—O)	3.400	
ν (C—H)	4.230	
ϕ (O—C—H)	0.380	0.350
ϕ (O—C—O)	1.200	0.750
ϕ (H—C—H)	0.225	0.250
ϕ (C—O—C)	1.200	0.750
ω (CH)	0.200	
τ(C—O)	0.400	

Vibrational modes

The asymmetric and symmetric C—H stretching's of CH_2 group were calculated at 2996 and 2919 cm^{-1} showing good agreement with the observed frequencies at 2985 and 2921 cm^{-1}, respectively.

The scissoring of CH_2 group is calculated at 1467 cm^{-1} and observed at 1472 cm^{-1} in FTIR. In IR and Raman spectra reported by previous workers,[7,13] the corresponding mode is observed at 1471 and 1493 cm^{-1}. Their calculated values are 1508 and 1506 cm^{-1}, respectively. Our results show a better agreement with the experimental data.

Two very intense bands have been observed at 1375 cm^{-1} and 1238 cm^{-1} in IR. Our theoretical calculations in this region show two frequencies at 1375 and 1245 cm^{-1}, respectively. According to the PEDs, both of them belong predominantly to (O—C—H) angle bend with a small contribution from (C—O) stretching vibrations.

The modes calculated at 1096 and 902 cm^{-1} correspond to the observed peaks at 1094 and 896 cm^{-1} in IR. For these bands, Raman scattering peaks are at 1091 and 932 cm^{-1}.[7] According to PED, these modes are mainly due to (C—O) stretching in combination with small contributions from (C—O) and (C—H) out of plane bendings.

Dispersion curves

The dispersion curves below 1500 cm^{-1} are shown in Figure 3(a). The modes above 1600 cm^{-1} are either nondispersive or their dispersion is less than 5 cm^{-1} hence dispersion curves in this region are not given.

One of the characteristic features of the dispersion curves is the convergence observed between some neighboring modes. They are far separated at the zone center but move closer at the zone boundary. For example, the two modes calculated at 1245 and 1095 cm^{-1} are separated by 150 wave numbers at the zone center, but at the zone boundary they are separated by 19 wave numbers only. Detailed PEDs of both modes at different δ values are shown in Table IV. This convergence arises mainly because of the closer sharing of potential energy in different measures by the various modes.

Another specific feature of the dispersion curves is the repulsion and mixing of the character of various pairs of modes. The mixing of character depends on the strength of coupling; stronger coupling

TABLE III
Normal Modes of Polyoxymethylene

Cal.	Obs.	Assignment (% potential energy distribution) δ = 0.0	Cal.	Obs.	Assignment (% potential energy distribution) δ = 0.9π (helix angle)
2996	2985	ν (C—H)(99)	2996	2985	(C—H)(99)
2920	2921	ν (C—H)(99)	2927	2921	ν (C—H)(99)
1466	1472	ϕ (H—C—H)(56) + ϕ (O—C—H)(23) + ω (CH)(9) + ν (C—O)(8)	1490	1472	ϕ (H—C—H)(46) + ϕ (O—C—H)(22) + ν (C—O)(12) + ω (CH)(12)
1375	1375	ϕ (O—C—H)(67) + ν (C—O)(24)	1363	1375	ϕ (O—C—H)(73) + ν (C—O)(18) + ϕ (H—C—H)(6)
1245	1238	ϕ (O—C—H)(92)	1217	1238	ϕ (O—C—H)(60) + ϕ (C—O—C)(27) + ν (C—O)(15) + ϕ (H—C—H)(7)+
1096	1094	ν (C—O)(49) + ϕ (O—C—H)(38) + τ (C—O)(7) + ω (CH)(5)	1203	1215[a]	ϕ (O—C—H)(70) + ϕ (O—C)(12) + ν (C—O)(8)
956	940	ϕ (O—C—H)(44) + ν (C—O)(40) + ω (CH)(10)	1087	1094	ν (C—O)(56) + ϕ (O—C—O)(25) + ϕ (O—C—H)(10) + τ (C—O)(7)
902	896	ν (C—O)(64) + ϕ (O—C—O)(14) + ϕ (O—C—H)(13)	906	896	ν (C—O)(69) + ϕ (O—C—H)(25)
625	626	ϕ (C—O—C)(55) + ϕ (O—C—O)(37)	739	744[a]	ϕ (O—C—O)(54) + ν (C—O)(30) + τ (C—O)(9) + ϕ (O—C—H)(5)
445	452	τ (C—O)(85) + ϕ (O—C—H)(7) + ν (C—O)(6)	561	564[a]	ϕ (C—O—C)(54) + ϕ (O—C—H)(27) + τ (C—O)(10) + ω (CH)(8)

Note: All frequencies are in cm^{-1}.
[a] Marked observed values are obtained from the regions of high density of states at helix angle.

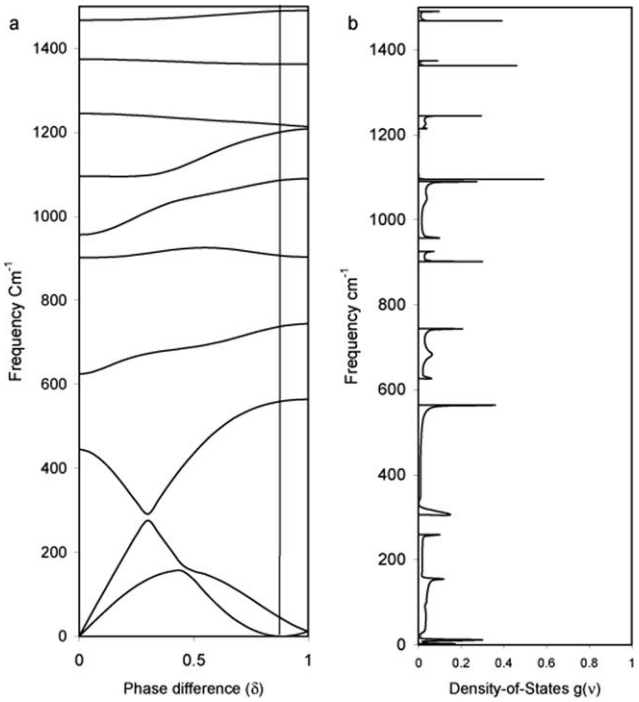

Figure 3 (a) Dispersion curves of polyoxymethylene in the range (0–1600 cm^{-1}). (b) Density-of-states of polyoxymethylene in the range (0–1600 cm^{-1}).

implies greater dispersion. This feature is observed among the three modes out of them two are acoustic (i.e., $\nu = 0$ at $\delta = 0$) and the third one shows a value equal to 445 at $\delta = 0.0$. On increasing the delta value, the mode calculated at 445 cm^{-1} goes on decreasing and the calculated value of two acoustic modes goes on increasing. At $\delta = 0.25\pi$ they become

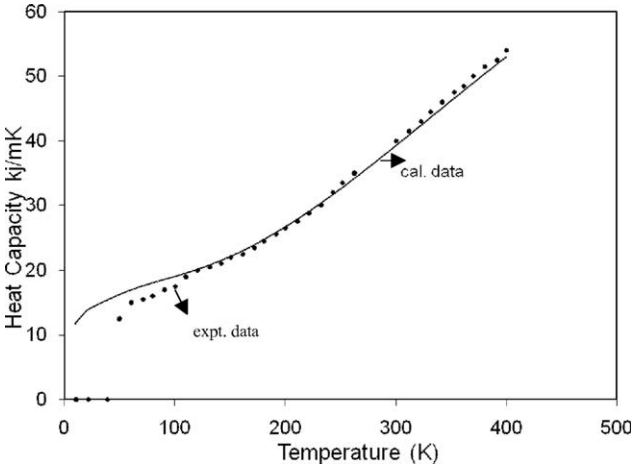

Figure 4 Variation of heat capacity with temperature for polyoxymethylene.

291, 276, and 136, respectively. On further increasing the delta value, the mode at 445 cm^{-1} again starts increasing and the remaining two acoustic modes start coming closer to each other. At approximately $\delta = 0.65\pi$, the two acoustic modes show a slight repulsion and finally their value decreases and at $\delta = \pi$ they again attain a 0 value. The other mode goes on increasing and finally becomes 564 cm^{-1} at $\delta = 1.00\pi$. The detailed PED of the above modes at various delta values is given in Table III. It is very difficult to assign a definite reason for the increasing acoustic modes coming closer to each other with increase in δ. One can only say that the δ values at which repulsion occurs refers to some internal symmetry point in the energy momentum space. At

TABLE IV
Pairs of Modes Showing Specific Features of Dispersion Curves

δ = 0.0	Cal. value at δ = 0.25π	P.E.D. at δ = 0.25	Cal. value at δ = 0.65π	P.E.D. at δ = 0.25π	Cal. value at δ = 1.00π	P.E.D. at δ = 1.00π
1245	1096	ϕ (O—C—H)(44) + ν (C—O)(38) + τ (C—O) (7) + ω (CH) (7)	1166	ϕ (O—C—H)(53) + ϕ (C—O—C)(18) + ν (C—O)(10) + τ (C—O)(7) + ω (CH)(6)	1209	ϕ (O—C—H)(94)
1095	998	ν (C—O)(53) + ϕ (O—C—H)(27) +ϕ (C—O—C)(6)	1062	ν (C—O)(68) + ϕ (O—C—O)(18) + ϕ (O—C—H)(8)	1090	ν (C—O)(55) + ϕ (O—C—O)(25) + ϕ (O—C—H)(10) + τ (C—O)(7)
956	909	ν (C—O)(61) + ϕ (O—C—O)(18) + ϕ (O—C—H)(13)	923	ν (C—O)(64) + ϕ (O—C—H)(19) + ϕ (O—C—O)(99)	903	ν (C—O)(69) + ϕ (O—C—H)(26)
445	291	ϕ (C—O—C)(65) + τ (C—O)(24) + ϕ (O—C—O)(8)	403	ϕ (C—O—C)(56) + ϕ (O—C—O)(33) + ϕ (O—C—H)(6)	564	ϕ (C—O—C)(53) + ϕ (O—C—H)(27) + τ (C—O)(10) + ω (CH)(8)
0	276	τ (C—O)(48) + ϕ (O—C—O)(44)	171	τ (C—O)(968) + ϕ (O—C—O)(16) + ϕ (C—O—C)(13)	12	τ (C—O)(81) + ϕ (O—C—O)(16)
0	136	τ (C—O)(99)	156	τ (C—O)(97)	11	τ (C—O)(81)+ ϕ (C—O—C)(17)

these δ points, the modes cannot be characterized as normal modes and hence do not belong to one of the irreducible representations and hence beyond symmetry governance.

Heat capacity

The dispersion curves obtained for POM have been used to calculate the density-of-states and heat capacity as a function of temperature. The density-of-states are shown in Figure 3(b). The variation of heat capacity as a function of temperature along with experimental data reported by Pan et al. are shown in Figure 4. Our calculated values show good agreement with the experimental work except in the low frequency region.

It may be added here that the contribution from the lattice modes is bound to make a difference to the heat capacity because of its sensitivity to low frequency modes. However, so far we have solved the problem only for an isolated chain. The calculation of dispersion curves for a three dimensional system is extremely difficult. Interchain modes involving hindered translatory and rotatory motion will appear and the total number of modes will depend on the contents of the unit cell. It would not only make the dimensionality of the problem prohibitive but also bring in an enormous number of interactions which are difficult even to visualize much less to quantify. Thus, it makes the problem somewhat intractable. The interchain interactions which involve hydrogen bonding and nonbonded interactions significantly contribute to vibrational dynamics by way of perturbing dispersion of normal modes and thermodynamic behavior especially these involving torsional modes. They are generally of the same order of magnitude as the weak intrachain interactions. Their introduction would, at best, bring about crystal field splittings at the zone center or zone boundary depending on the symmetry dependent selection rules. However, the intrachain assignments will remain by and large undisturbed. Thus, in spite of several limitations involved in the calculation of specific heat, this work does provide a good starting point for further basic studies on thermodynamic behavior of polymers which go into well-defined conformations. Complete three dimenasional studies have been reported only on polyethylene and polyglycine[25,26] where the unit cell is small. Other calculations with approximate interchain interactions, as in a β sheet of polypeptides, are confined to calculations of zone center and zone boundary frequencies alone. This work goes beyond the calculations of the dispersion curves within the entire zone.

CONCLUSIONS

FTIR spectral data on POM can be well interpreted by solving the secular equation based on Wilson GF matrix method as modified by Higgs and using Urey Bradley force field. Some of the characteristic features such as repulsion are observed. These give rise to higher density-of-states. Nearly linear behavior of heat capacity with temperature shows the multiple uses to which Delrin can be put.

References

1. Eschbach, L. Int J Care Injured 2000, 31, 22.
2. Zhang, Y.; Zhou, L.; Li, D.; Xue, N.; Xu, X.; Li, J. Chem Phys Lett 2003, 376, 493.
3. Rodrigues, C. V. M.; Serricella, P.; Linhares, A. B. R.; Guerdes, R. M.; Borojevic, R.; Rossi, M. A.; Duarte, M. E. L.; Farin, M. Biomaterials 2003, 24, 4987.
4. Seal, B. L.; Otero, T. C.; Panitch, A. Mater Sci Eng 2001, 34, 147.
5. Wang, M. Biomaterials 2003, 24, 2133.
6. Toshio, U.; Tadakoro, H. J. Polym Sci Part A-2 1967, 5, 63.
7. Matsui, Y.; Kubota, T. J Polym Sci Part A 1965, 3, 2275.
8. Wunderlich, B. Pure Appl Chem 1995, 67, 6, 1019.
9. Dasgupta, S.; Smith K. A.; Goddard, W. A. J Phys Chem 1993, 97, 42, 10891.
10. Takasa, K.; Ishikawa, T.; Takeda, K.; Takeda, K. Jpn J Polym Sci Technol 2005, 62, 604.
11. Mohanraj, J.; Morawiec, J.; Pawlak, A.; Barton, D. C.; Galeski, A.; Ward, I. M. Polymer 2008, 49, 303.
12. Tashiro, K.; Kamae, T.; Asanaga, H.; Oikawa, T. Macromolecules 2004, 37, 826.
13. Sugeta, H.; Miyazawa, T.; Kajiura, T. 1968, 7, 251.
14. Sauer, B. B.; Mclean, R. S.; Londono, J. D.; Hsiao, B. S. J Macromol Sci 2000, 39, 519.
15. Samon, J. M.; Schultz, J. M.; Hsiao, B. S.; Khot, S.; Johnson, H. R. Polymer 2001, 42, 1547.
16. Vladimir A. B.; Egorova, L. M.; Egorov, V. M.; Peschanskaya, N. N.; Yakushev, P.N.; Keating, M. Y.; Flexman, E. A.; Kassal, R. A.; Schodt, K. P. Thermochim Acta 2002, 391, 227.
17. Takasa, K.; Miyashita, N.; Tachibana, S.; Takeda, K. J Soc Mater Sci 2005, 54, 51.
18. Samyn, S.; Driessche, I. V.; Schoukens, G. J Polym Res 2007, 14, 411.
19. Abdel-Hady, E. E.; Hamdy, Mohamed, F. M.; Fareed S. S. Radiat Phys Chem 2007, 76, 138.
20. Pielichowski, K.; Leszczynska, A. J Therm Analysis Calorim 2004, 78, 399.
21. Wilson, E. B.; Decius, J. C.; Cross, P. C. Molecular Vibrations: The Theory of Infrared and Raman Vibrational Spectra; New York; Dover Publication, 1980.
22. Higgs, P. W. Proc Roy Soc (London) 1953, A220, 472.
23. Tandon, P.; Gupta, V. D.; Prasad, O.; Rastogi, S.; Gupta, V. P. J Polym Sci Part B Polym Phys 1997, 35, 2281.
24. Pan, M.; Verma, N.; Wunderlich, B. J Therm Anal 1989, 35, 955.
25. Tasumi, M.; Krimm, S. J Chem Phys 1967, 46, 755.
26. Tasumi, M.; Shimanouchi, J. Chem Phys 1965, 43, 1245.